European Journal of Medicinal Chemistry 198 (2020) 112392

Contents lists available at ScienceDirect

European Journal of Medicinal Chemistry

journal homepage: http://www.elsevier.com/locate/ejmech

Research paper

Synthesis, characterization and carbonic anhydrase I and II inhibitory evaluation of new sulfonamide derivatives bearing dithiocarbamate

Begüm Nurpelin Sağlık [a, b, *], Derya Osmaniye [a, b], Ulviye Acar Çevik [a, b], Serkan Levent [a, b], Betül Kaya Çavuşoğlu [c], Oya Büyükemir [d], Deniz Nezir [d], Abdullah Burak Karaduman [e], Yusuf Özkay [a, b], Ali Savaş Koparal [f], Şükrü Beydemir [d], Zafer Asım Kaplancıklı [a]

[a] Department of Pharmaceutical Chemistry, Faculty of Pharmacy, Anadolu University, 26470 Eskişehir, Turkey
[b] Doping and Narcotic Compounds Analysis Laboratory, Faculty of Pharmacy, Anadolu University, 26470 Eskişehir, Turkey
[c] Department of Pharmaceutical Chemistry, Faculty of Pharmacy, Zonguldak Bülent Ecevit University, 67600 Zonguldak, Turkey
[d] Department of Biochemistry, Faculty of Pharmacy, Anadolu University, 26470 Eskişehir, Turkey
[e] Department of Pharmaceutical Toxicology, Faculty of Pharmacy, Anadolu University, 26470 Eskişehir, Turkey
[f] Open Education Faculty, Anadolu University, 26470 Eskişehir, Turkey

ARTICLE INFO

Article history:
Received 18 March 2020
Received in revised form
16 April 2020
Accepted 25 April 2020
Available online 4 May 2020

Keywords:
Carbonic anhydrase
Cytotoxicity
Dithiocarbamate
Molecular docking
Sulfonamide

ABSTRACT

In this study, novel dithiocarbamate-sulfonamide derivatives (**3a**-**3k**) were synthesized to investigate their inhibitory activity on purified human carbonic anhydrase (*h*CA) I and II. The IC_{50} and K_i values of the compounds were calculated to compare their inhibition profiles on *h*CA I and II isoenzymes. Acetazolamide was used as the standard inhibitor in the enzyme inhibition assay. Compounds **3a**, **3e**, **3g**, **3h**, **3j** and **3k** showed notable inhibitory effects against *h*CA I and II. Among these compounds, compound **3h** was found to be the most active derivate against both the *h*CA I and II enzymes with K_i values of 0.032 ± 0.001 μM and 0.013 ± 0.0005 μM, respectively. The cytotoxicity of compounds **3a**, **3e**, **3g**, **3h**, **3j** and **3k** toward NIH/3T3 (mouse embryonic fibroblast cell line) was observed and the compounds were found to be non-cytotoxic. Furthermore, molecular docking studies were performed to investigate the interaction types between compound **3h** and the *h*CA I and II enzymes. As a result of this study a novel and potent class of CA inhibitors with good activity potential were identified.

1. Introduction

Carbonic anhydrases (CAs) are a superfamily of metalloenzymes that are involved in the fundamentals of biochemical processes in which carbon dioxide reversibly passes protons to bicarbonate. CAs are classified into seven genetically distinct families. Only the α-class is exclusively present in humans which is further distinguished by 16 different *h*CA isoforms. Some of these isoforms are cytosolic (CA I, CA II, CA III, CA VII, CA XIII), some are membrane-bound (CA IV, CA IX, CA XII, CA XIV and CA XV), some are mitochondrial (CA VA and CA VB) and CA VI is secreted in saliva and milk. These CA isoforms play a vital role in various physiological processes such as carboxylation, ureagenesis, photosynthesis, respiration, and various biochemical processes including calcification, pH regulation, bone resorption etc. all of which are directly or indirectly associated with CO_2 hydration reaction. Abnormal activities or levels of these enzymes are associated with many human disorders. Therefore, it is important to develop an effective approach that can selectively inhibit the isoforms involved in different diseases. CA inhibitors (CAIs) are used to treat many diseases, including various neurological disorders, glaucoma, acid-base disequilibria, and gastroduodenal ulcers [1–9].

It has been reported that sulfonamides ($R-SO_2NH_2$) are a significant class of chemicals that possess the potency to inhibit the CA isoenzymes involved in diverse physiological and pathological processes such as antimicrobial, anti-HIV, antifungal, antibacterial, antidiabetic, anticonvulsant, anticancer. Additionally, sulfonamide derivatives are potent CAIs. These compounds bind to the active site of CAs via an interaction between the catalytic zinc ion of the enzyme and the deprotonated nitrogen of the sulfonamide moiety and block the enzymatic activity of CA. Recent studies in the literature has also shown the potential CA inhibitory activity of

* Corresponding author. Anadolu University, Faculty of Pharmacy, Department of Pharmaceutical Chemistry, 26470, Eskişehir, Turkey.
E-mail address: bnsaglik@anadolu.edu.tr (B.N. Sağlık).

https://doi.org/10.1016/j.ejmech.2020.112392
0223-5234/

sulfonamide compounds [10–20].

Dithiocarbamates (DTCs), which were recently discovered to be CA inhibitors, have a wide range of application areas from agriculture to medicine. DTCs are well known metal complexing agents that DTCs can also form complexes containing a wide variety of transition metal ions in various oxidation modes owing to the absence of anionic CS_2 moiety. With the help of this inorganic anion, the CS_2^- moiety was detected as a new zinc binding group (ZBG) in the design of CAIs [21–24].

For these reasons, in this study a new CAIs was developed. In this context, sulfonamide and dithiocarbamate moieties, which were selected due to studies showing that both of them displayed CAI activity, were synthesized and the effect of compounds containing these two systems on CAs was investigated.

2. Result and discussion

2.1. Chemistry

The synthetic route to the target compounds **3a-3k** are presented in Scheme 1. Initially, 2-chloro-*N*-(4-sulfamoylphenyl)acetamide (**1**) was obtained using an acetylation reaction. Secondly, the dithiocarbamate derivatives (**2a-2k**) were obtained as a result of a reaction between the carbonsulfide and secondary amines. Finally, the dithiocarbamate derivatives (**2a-2k**) and acetylated product (**1**) were reacted to obtain the target compounds. The structure of the obtained compounds were elucidated by spectroscopic analyses (^{1}H NMR, ^{13}C NMR and HRMS). In the ^{1}H NMR spectrum, methylene protons (-CH_2-) were observed between 4.29 ppm and 4.34 ppm as singlet. The amino protons of the sülfonamide gave peak between 7.24 ppm and 7.26 ppm as singlet. The 1,4-disubstituted benzene ring to which the sulfonamide group was attached gave peaks between 7.72 ppm and 7.79 ppm. The amide protons gave peaks between 10.60 ppm and 10.76 ppm. In the ^{13}C NMR spectrum, carbonyl carbons were recorded between 166.34 ppm and 166.44 ppm, while thiocarbonyl carbons were recorded between 194.41 ppm and 195.34 ppm. In the HRMS, all masses were matched well with the expected M + H values.

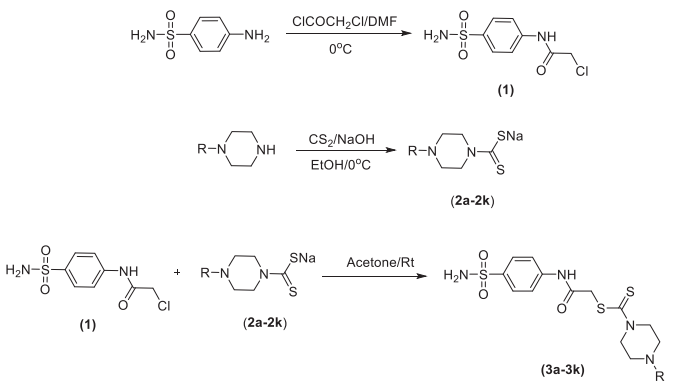

Compounds	R
3a	Methyl
3b	Cyclohexyl
3c	4-Nitrophenyl
3d	4-Fluorobenzyl
3e	4-Methylbenzyl
3f	4-Methoxybenzyl
3g	2-(Dimethylamino)ethyl
3h	3-(Dimethylamino)propyl
3i	Furan-2-carbonyl
3j	Pyridin-2-yl
3k	Pyrimidin-2-yl

Scheme 1. Synthesis way of the compounds **3a-3k**.

2.2. Biological activity

2.2.1. Enzyme inhibition

The capability of compounds (**3a-3k**) in inhibiting two physiologically relevant *h*CA isoforms, namely *h*CA I and II, was assessed. The inhibition data (IC_{50} and K_i) of the prepared compounds and the standard inhibitor acetazolamide (AZA) against *h*CA isoforms are summarized in Table 1. For *h*CA I enzyme, IC_{50} values were calculated between 0.0.47 and 87.439 μM, however IC_{50} values were obtained in 0.024–91.395 μM range for *h*CA 2 enzyme. Also, these IC_{50} plots, which were gained by regression analysis, are presented in Figs. 1 and 2. The K_i values of the compounds against *h*CA I were found to be between 0.032 μM and 64.770 μM, whereas the K_i values against *h*CA II were found to be in the range of 0.013 μM–67.700 μM. Compounds **3a**, **3e**, **3g**, **3h**, **3j** and **3k** showed notable inhibitory effects against both *h*CA I and II. Among these compounds, compound **3h** was determined as the most active derivate against both the *h*CA I and II enzymes with K_i values of 0.032 ± 0.001 μM and 0.013 ± 0.0005 μM, respectively. In addition, it was observed that this compound had a selective inhibition profile on *h*CA II.

Compounds **3a**, **3g** and **3j** were the other derivates active on *h*CA II enzyme after compound **3h.** Compound **3j** was especially important when making comparisons with the previous study conducted by the authors of the present study, in which.it was reported that the pyridine ring contributed to *h*CA II inhibition [13]. The present study also supported this information. Furthermore, the dithiocarbamate group entering the structure increased activity by about 10-fold (K_i value of compound **3j** is 0.028 μM) compared to the previous compound (2-(2-(Pyridin-3-ylmethylene)hydrazinyl)-*N*-(4-sulfamoylphenyl) acetamide (K_i = 0.288 μM)).

In addition, it was determined that methyl (**3a**), dimethylaminoethyl (**3g**) and dimethylaminopropyl (**3h**) substituents contributed positively to the enzyme inhibition profile of *h*CA II. It was thought that extended alkyl chains potentiated enzyme inhibition. On the other hand, compounds bearing substituted phenyl and benzyl rings had lower enzyme activity, which indicated that the entering benzene ring decreased activity.

2.2.2. Enzyme kinetic studies

The enzyme kinetic studies of all synthesized compounds (**3a-3k**) on both the *h*CA I and II enzymes were carried out in order to determine the inhibition type and calculate the K_i values. The inhibition types are divided into two as reversible inhibition, comprised of the uncompetitive, competitive, non-competitive and mixed type inhibitions subtypes, and irreversible inhibition. All of these subtypes of inhibition can be determined with Lineweaver-Burk plots according to the style of the graphics [13,25].

The Lineweaver-Burk plots of the most active compound, namely **3h**, on the *h*CA I and II enzymes are presented in Figs. 3 and 4. It can be seen from these figures, that compound **3h** showed non-competitive inhibition type against both isoenzymes as the relevant Lineweaver-Burk plots had the same intercept on x-axis and diverse slopes and intercepts on y-axis in the graphics.

2.2.3. Cytotoxicity

According to the general medicinal chemistry approach, a drug candidate should show biological activity but not be toxic. Therefore, in order to evalaute the cytotoxicity profiles of the most active derivatives, compounds **3a**, **3e**, **3g**, **3h**, **3j** and **3k** were screened by

Table 1
IC_{50} and K_i values (μM) of the compounds **3a-3k** on human CA isoenzymes (*h*CA I and II).

Compounds	IC_{50} (μM)		K_i (μM)	
	*h*CA I	*h*CA II	*h*CA I	*h*CA II
3a	0.152 ± 0.007	0.028 ± 0.001	0.098 ± 0.003	0.021 ± 0.001
3b	20.805 ± 0.853	0.522 ± 0.021	11.583 ± 0.536	0.360 ± 0.015
3c	21.326 ± 0.832	2.234 ± 0.091	11.887 ± 0.498	2.027 ± 0.099
3d	0.415 ± 0.017	0.251 ± 0.011	0.299 ± 0.012	0.180 ± 0.008
3e	0.375 ± 0.014	0.131 ± 0.005	0.280 ± 0.011	0.087 ± 0.003
3f	87.439 ± 3.061	91.395 ± 3.380	64.770 ± 2.547	67.700 ± 2.988
3g	0.081 ± 0.003	0.033 ± 0.013	0.049 ± 0.002	0.026 ± 0.001
3h	**0.047 ± 0.002**	**0.024 ± 0.001**	**0.032 ± 0.001**	**0.013 ± 0.0005**
3i	9.564 ± 0.411	0.857 ± 0.033	7.713 ± 0.380	0.597 ± 0.025
3j	0.281 ± 0.011	0.039 ± 0.001	0.164 ± 0.007	0.028 ± 0.001
3k	0.065 ± 0.002	0.191 ± 0.008	0.041 ± 0.002	0.107 ± 0.004
Acetazolamide	0.361 ± 0.014	0.175 ± 0.007	0.289 ± 0.010	0.135 ± 0.004

using MTT assay on healthy NIH/3T3 (mouse embryonic fibroblast) cell lines (ATCC CRL1658) [26].

Table 2 presents the IC_{50} (μM) values of these compounds against the NIH/3T3 cell line. It can be seen that these IC_{50} values (14.472 - >1000 μM) were higher than those obtained in the inhibition assay for the *h*CA I and II enzymes (0.280−0.013 μM). Consequently, these compounds were found to be non-toxic in their effective concentration against the *h*CA I and II enzymes.

2.3. Molecular docking

According to the enzyme inhibition assay, compound **3h** was found to be the most active derivative against the *h*CA I and II enzymes. Docking studies were performed in order to gain more insight into the binding modes of this compound to evaluate the effects of structural modifications on the inhibitory activity against *h*CA I and II. The X-ray crystal structures of *h*CA I (PDB ID: 1AZM) [27] and *h*CA II (PDB ID: 3HS4) [28] were obtained from the Protein Data Bank server (www.pdb.org). The docking poses of compound **3h** are presented in Figs. 5–12.

According to the docking poses, the sulfonamide groups of compound **3h** were in N-deprotonated form, which serves as a zinc-binding site and thus, this compound could expectedly bind to the active sites of the enzymes with its sulfonamide groups coordinated to the zinc ion [29]. The amino groups and one of the oxygen atoms of the deprotonated sulfonamide groups bonded to the Zn^{+2} ion by salt bridge and a metal coordination bond, respectively. The other oxygen atom of the deprotonated sulfonamide group created a hydrogen bond with the amino of Thr199 of compound **3h** on both the *h*CA I and II isoenzymes. Both of these interactions were typical for all sulfonamide-CA complexes investigated so far [29–34].

When the docking poses of compound **3h** on the *h*CA I and II enzymes were analyzed, it was seen that certain functional groups in the compound showed interaction in both enzyme active sites. The phenyl ring in the chemical structure was in an π-π interaction with imidazole rings of Hid200 of the *h*CA I enzyme and with Hid94 of the *h*CA II enzyme. The hydrogen bond was observed between the carbonyl of the amide group and the amino of Gln92 on the *h*CA I enzyme active site and between the carbonyl and the amino of groups of Asn62 and Asn67 on the *h*CA II enzyme active site. The last interaction observed was related to the dimethylaminopropyl group, which was thought to have caused the higher enzyme activity. For the *h*CA I enzyme, the nitrogen atom of this group formed a salt bridge with Asp72 amino acid residue and created a hydrogen bond with the carbonyl of Asp72.

It can be seen from Figs. 7, 8, 11 and 12 that the van der Waals and electrostatic interactions provided stronger binding to the enzyme active sites of *h*CA I and II for compound **3h**. On the *h*CA I enzyme active site, this compound showed favorable van der Waals interactions with Phe91, Gln92, Hid94, Hid96, Leu131, Val143, Leu198, Thr199, Hid200 and Trp209. On the *h*CA II enzyme active site, the same compound, showed van der Waals interactions with Asn67, Ile91, Gln92, Hid96, Hid119, Val121, Phe131, Leu198, Thr199 and Thy200, which were displayed in pink and red colours as described in the user guide of Glide [35]. It was thought that the phenyl and piperazine rings and the amide and dithiocarbamate moieties enhanced the van der Waals interactions with the enzyme active region. Furthermore, compound **3h** showed promising electrostatic contributions with Gln92, Hid94, Hid96, Glu106 and Hid119 for both the *h*CA I and II enzymes.

As mentioned in the enzyme inhibition assay, compound **3h** was the most active derivative against the *h*CA I and II enzymes with K_i values of 0.032 ± 0.001 μM and 0.013 ± 0.00050.176 μM, respectively. The structurally common feature of this compound was determined to be the dimethylaminopropyl group near to the piperazine ring. In this context, the docking studies supports the enzyme inhibition assay results. The interactions related to the dimethylaminopropyl group were important in terms of explaining the inhibitory activities of compound **3h**. The docking results showed that extended carbon chain enhances the van der Waals interactions with the amino acids in the active site and intensified the proper bonding. In addition, compound **3h** demonstrated additional interactions as a result of its amino in the dimethylaminopropyl group. Consequently, this difference influenced and explained the binding capability of compound **3h** to the enzyme active sites of *h*CAI CA II and its enzyme inhibition potencies towards these enzymes.

3. Conclusion

In conclusion, a new series of dithiocarbamate-sulfonamide derivatives were designed and their biological activity for the inhibition of CA isozymes was evaluated. According to the IC_{50} and K_i values, compound **3h**, which contained a dimethylaminopropyl alkyl chain, was found to be the most effective compound against both *h*CA I and II. Enzyme inhibition studies have an important place in drug design development and research in the field of pharmaceutical chemist. Therefore, these findings showed that the new sulfonamide derivatives inhibited *h*CA I and II enzyme activity and suggested that sulfonamide derivatives could be improved in future studies.

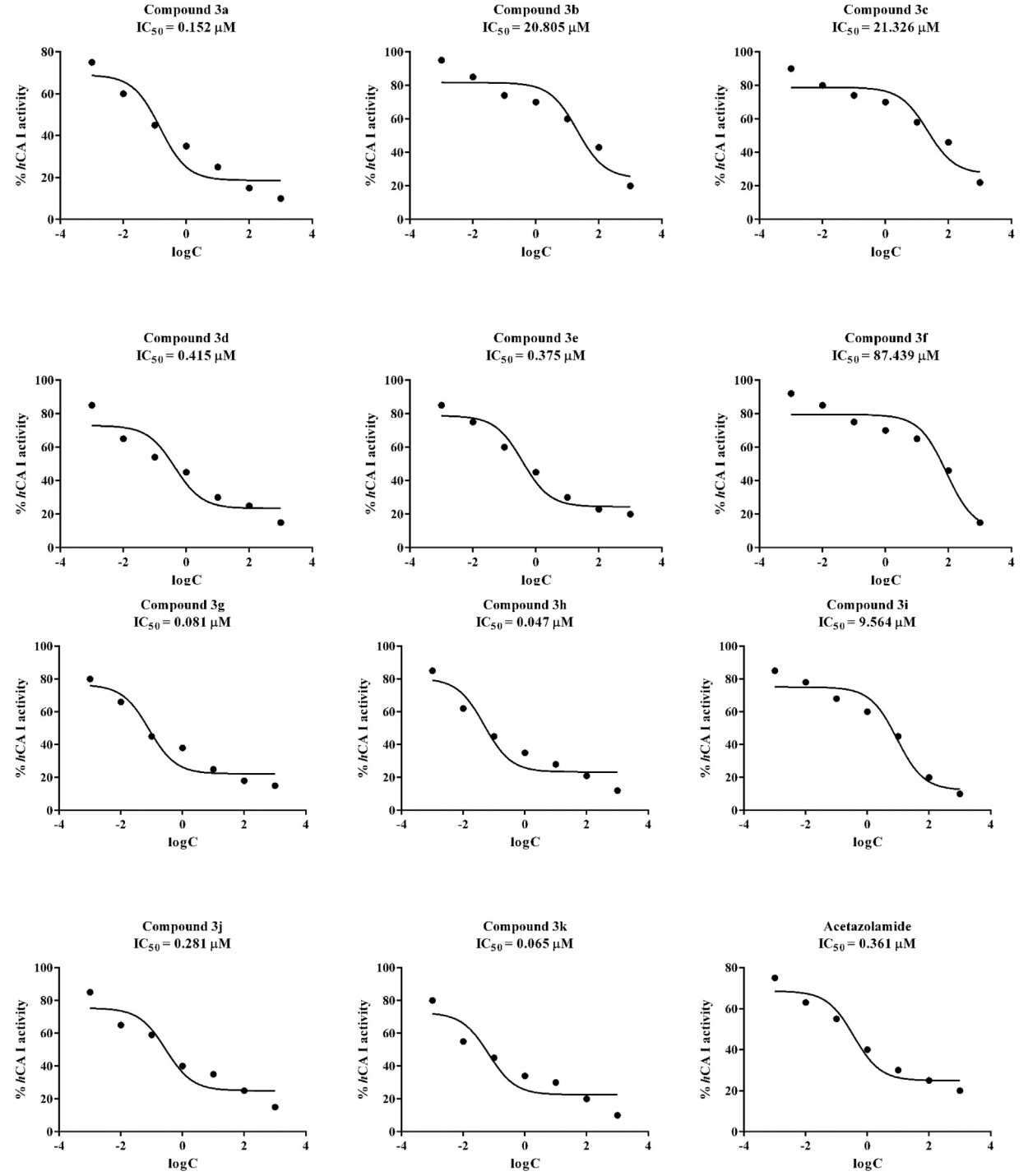

Fig. 1. IC_{50} plots of compounds **3a**-**3k** and acetazolamide on esterase activity for *h*CA I enzyme (The graphs are formed using *GraphPad Prism Version 6* via regression analyses).

4. Experimental

4.1. Chemistry

All of the chemicals employed in the synthetic procedures in this study were purchased from Sigma-Aldrich Chemicals (Sigma-Aldrich Corp., St. Louis, MO, USA) or Merck Chemicals (Merck KGaA, Darmstadt, Germany). The melting points of the obtained compounds were determined with a MP90 digital melting point apparatus (Mettler Toledo, OH, USA) and were uncorrected. The IR spectra were obtained on an IR Prestige-21 (Shimadzu, Tokyo, Japan). The ^{1}H NMR and ^{13}C NMR spectra of the synthesized compounds were registered with Bruker 300 MHz and 75 MHz digital FT-NMR spectrometers (Bruker Bioscience, Billerica, MA, USA) in DMSO-d_6, respectively. The splitting patterns in the NMR spectra were designated as follows: s: singlet; d: doublet; t: triplet; m: multiplet. The coupling constants (J) were reported as Hertz. The M+1 peaks were determined by Shimadzu LC/MS ITTOF system

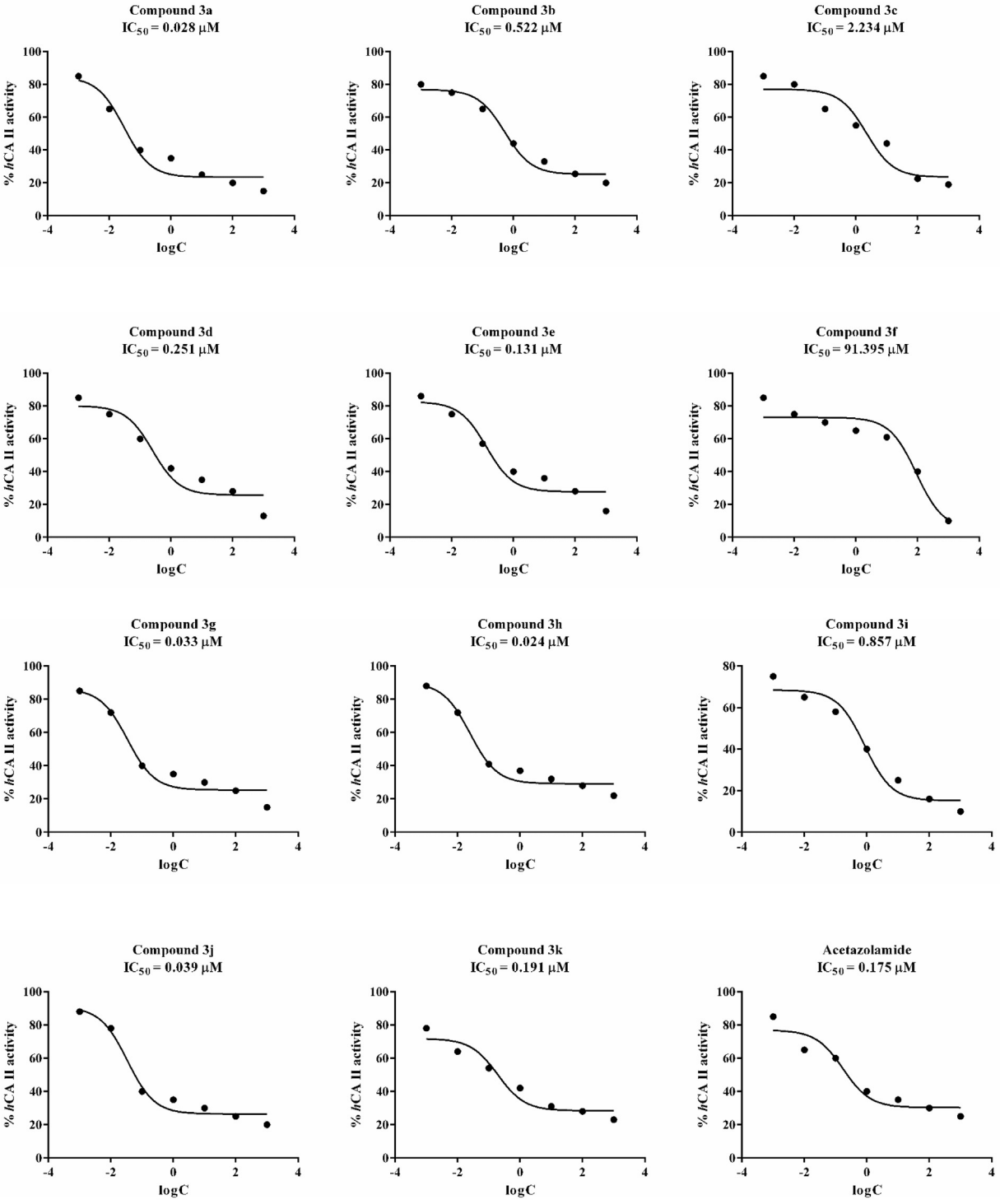

Fig. 2. IC_{50} plots of compounds **3a**-**3k** and acetazolamide on esterase activity for *h*CA II enzyme (The graphs are formed using *GraphPad Prism Version 6* via regression analyses).

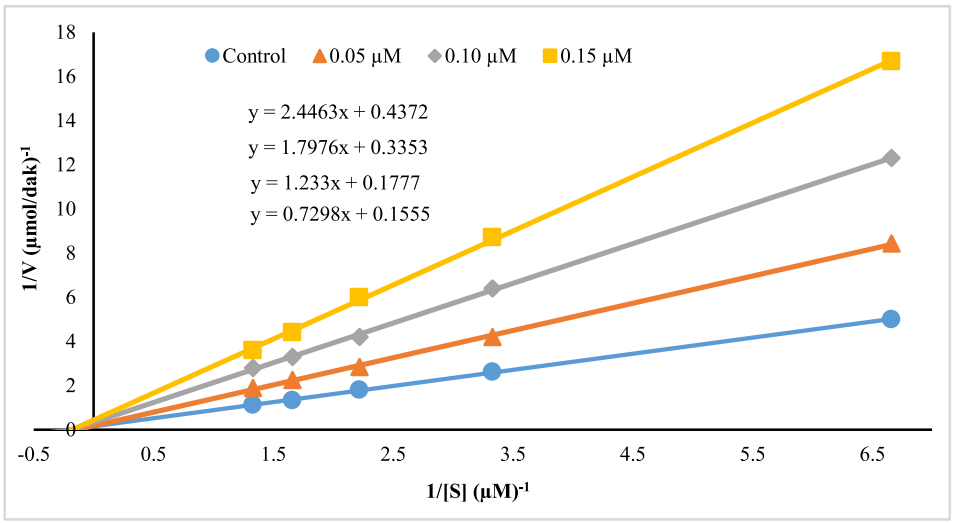

Fig. 3. Lineweaver–Burk graphs of the compound **3h** on *h*CA I.

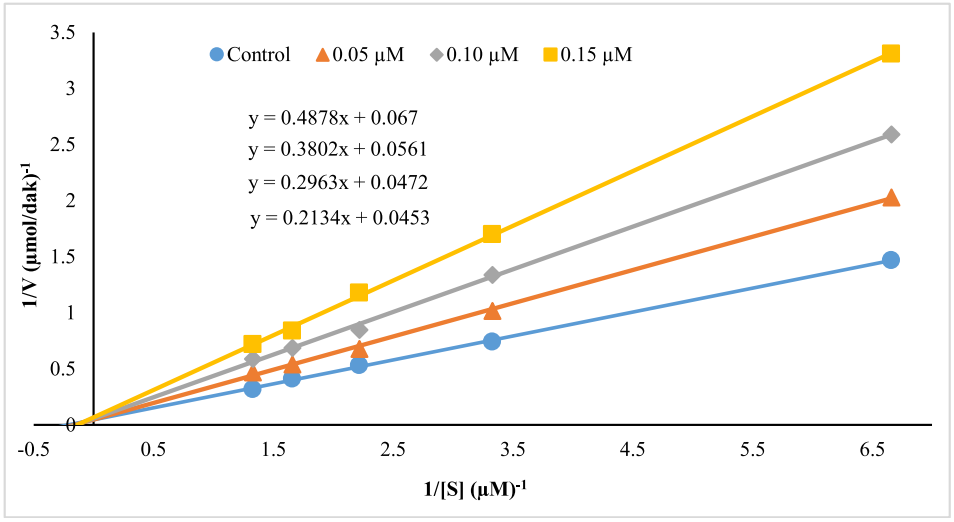

Fig. 4. Lineweaver–Burk graphs of the compound **3h** on *h*CA II.

Table 2
IC_{50} (µM) values of the compounds **3a**, **3e**, **3g**, **3h**, **3j** and **3k** derivatives against NIH/3T3 cell line.

Compounds	3a	3e	3g	3h	3j	3k
IC_{50} (µM)	14.472 ±0.433	58.064 ±1.104	>1000	>1000	18.477 ±0.397	16.525 ±0.287

(Shimadzu, Tokyo, Japan). All reactions were monitored by thin-layer chromatography (TLC) using Silica Gel 60 F254 TLC plates (Merck KGaA, Darmstadt, Germany).

4.1.1. General procedure for the synthesis of the compounds

*4.1.1.1. Synthesis of 2-chloro-N-(4-sulfamoylphenyl)acetamide (**1**).* For the synthesis of the 2-chloro-*N*-(4-sulfamoylphenyl)acetamide, 4-aminobenzenesulfonamide (0.06 mol, 10.1 gr) were dissolved in dimethylformamide (20 mL). The mixture was cooled in an ice bath and chloroacetyl chloride (0.07 mol, 5.8 mL) was added dropwise with stirring. Then, the reaction mixture was stirred for 1h at room temperature. The reaction content was poured into iced-water and the precipitated product was washed with water, filtered, dried, and then recrystallized from EtOH.

*4.1.1.2. Synthesis of dithiocarbamate derivatives (**2a**-**2k**).* For the synthesis of the dithiocarbamate derivatives (**2a**-**2k**), a mixture of carbondisulfide in ethanol was added to a mixture of appropriate piperazine (0.22 mol, 3.73 g) and NaOH in EtOH (30 mL) and stirred in an ice-bath for 2h. After the reaction was complete, the precipitated product was filtered, washed with diethylether and dried.

*4.1.1.3. General procedure for the synthesis of target compounds (**3a**-**3k**).* For the synthesis of the target compounds (**3a**-**3k**), 2-chloro-*N*-(4-sulfamoylphenyl)acetamide (**1**) (0.83 mmol) and the appropriate dithiocarbamate derivatives were stirred for 4h in acetone. After the reaction was complete, the acetone was evaporated under reduced pressure. The precipitated product was washed with water in order to remove the sodium chloride and then dried and recrystallized from EtOH.

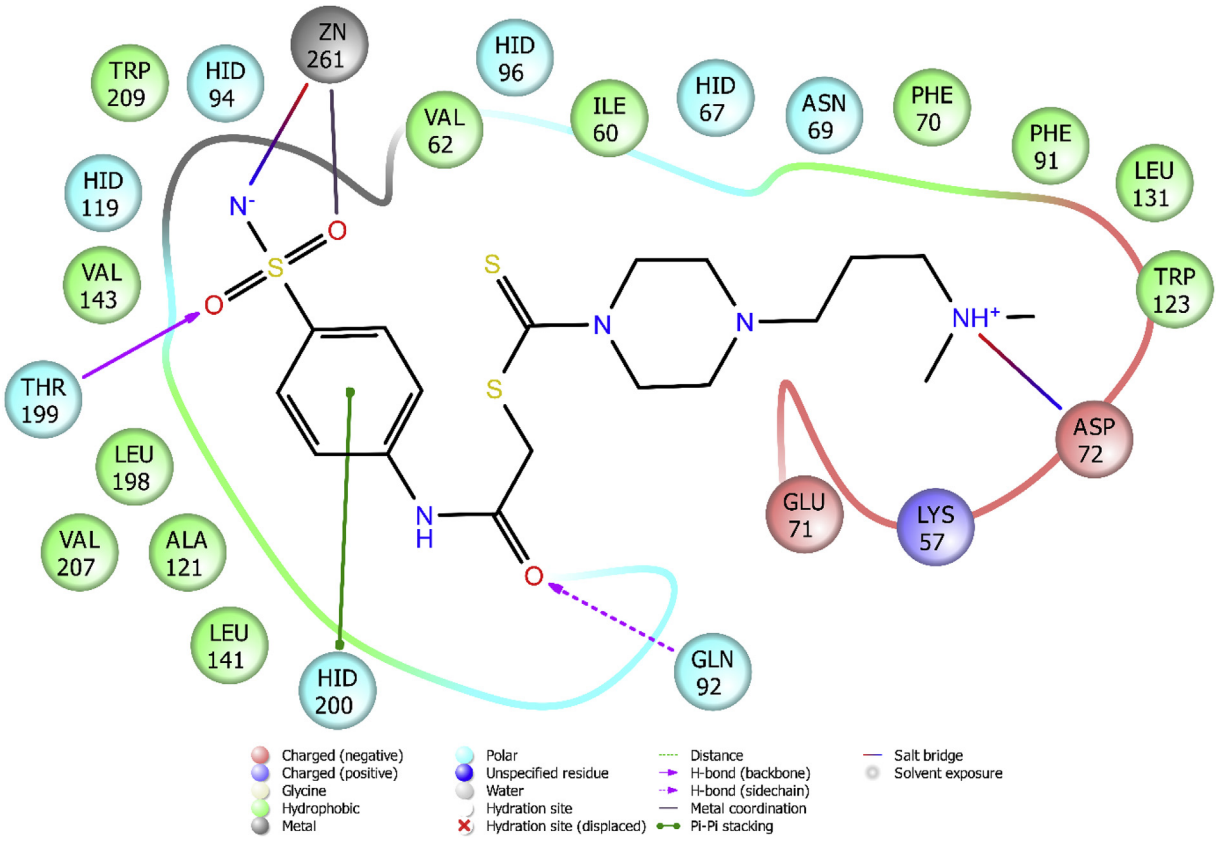

Fig. 5. Two-dimensional interaction mode of compound **3h** in the enzyme active site of *h*CA I (CA I PDB Code: 1AZM).

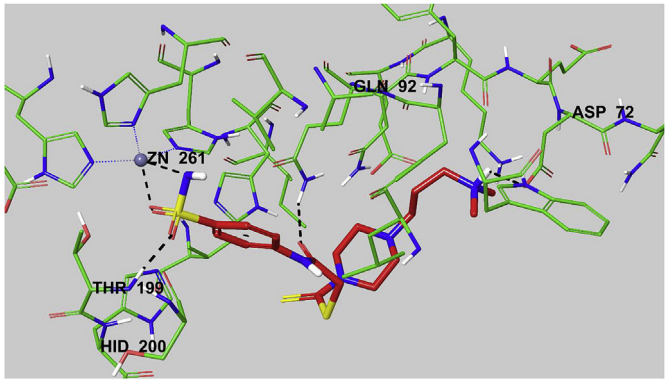

Fig. 6. The interacting mode of compound **3h** in the active region of *h*CA I. The inhibitor and the important residues in the active site of the enzyme are presented by tube model. The inhibitor is colored with red, whereas the residues are lime green.

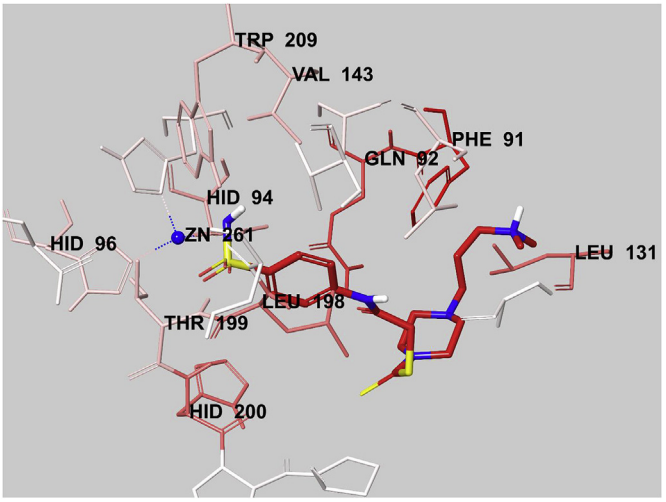

Fig. 7. The van der Waals interaction of compound 3h with active region of hCA I. The active ligand has a lot of favorable van der Waals interactions (red and pink). (For interpretation of the references to color in this figure legend, the reader is referred to the Web version of this article.)

4.1.1.3.1. 2-Oxo-2-((4-sulfamoylphenyl)amino)ethyl 4-methylpiperazine-1-carbodithioate (***3a***). Yield: 85%, M.P. = 208–210 °C. ^{1}H NMR (300 MHz, DMSO-d_6): δ = 2.22 (3H, s, $-CH_3$), 2.39–2.42 (4H, m, piperazine), 3.96 (2H, br.s., piperazine), 4.20 (2H, br.s., piperazine), 4.29 (2H, s, $-CH_2$-), 7.25 (2H, s, $-SO_2NH_2$), 7.75 (4H, d, J = 2.8 Hz, 1,4-Disubstitutedbenzene), 10.61 (1H, br.s., −NH). ^{13}C NMR (75 MHz, DMSO-d_6): δ = 41.68, 45.56, 50.20, 51.54, 54.43, 119.06, 127.20, 138.90, 142.34, 166.42, 194.84. HRMS (m/z): $[M+H]^+$ calcd for $C_{14}H_{20}N_4O_3S_3$: 389.0770; found: 389.0767.

4.1.1.3.2. 2-Oxo-2-((4-sulfamoylphenyl)amino)ethyl 4-cyclohexylpiperazine-1-carbodithioate (***3b***). Yield: 88%, M.P. = 200–201 °C. ^{1}H NMR (300 MHz, DMSO-d_6): δ = 1.06–1.19 (5H, m, cyclohexyl), 1.55–1.59 (1H, m, cyclohexyl), 1.73–1.76 (4H, m, cyclohexyl), 2.29 (1H, m, cyclohexyl), 2.58 (4H, br.s., piperazine), 3.92 (2H, br.s., piperazine), 4.17 (2H, br.s., piperazine), 4.29 (2H, s, $-CH_2$-), 7.24 (2H, s, $-SO_2NH_2$), 7.74 (4H, d, J =2.6 Hz, 1,4-Disubstitutedbenzene), 10.60 (1H, br.s., −NH). ^{13}C NMR (75 MHz, DMSO-d_6): δ = 25.69, 26.27, 28.77, 41.62, 48.59, 50.86, 52.18, 62.72,

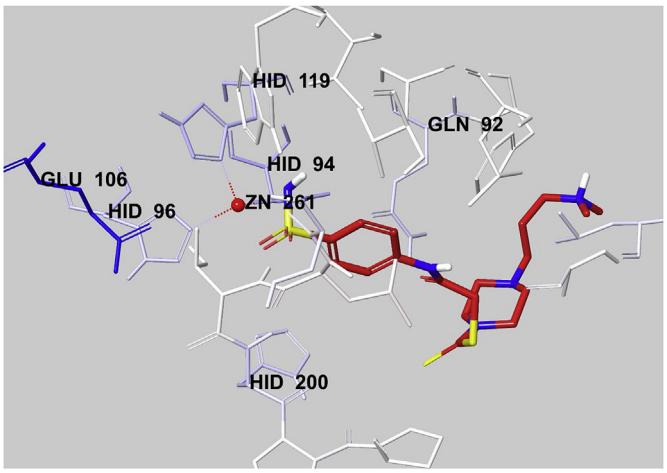

Fig. 8. The electrostatic interaction of compound **3h** with active region of *h*CA I. The residues are colored (blue and light blue) according to the distance from ligand by Per-Residue Interaction panel.

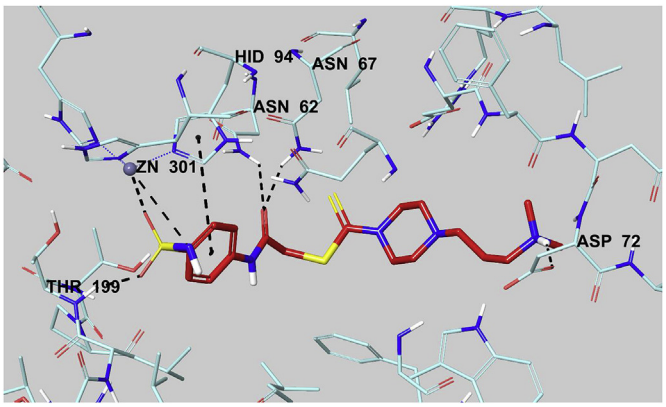

Fig. 10. The interacting mode of compound **3h** in the active region of *h*CA II. The inhibitor and the important residues in the active site of the enzyme are presented by tube model. The inhibitor is colored with red, whereas the residues are turquoise.

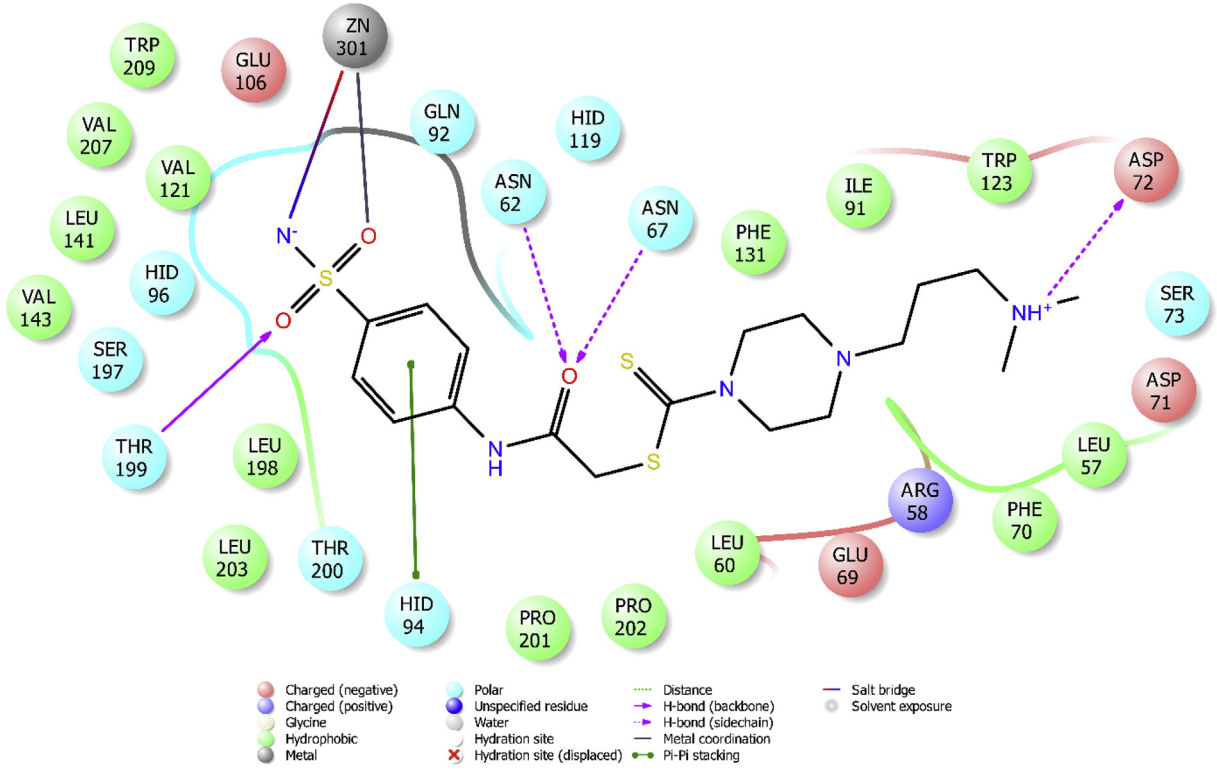

Fig. 9. Two-dimensional interaction mode of compound **3h** in the enzyme active site of *h*CA II (CA II PDB Code: 3HS4).

119.05, 127.19, 138.90, 142.34, 166.44, 194.41. HRMS (*m*/*z*): $[M+H]^+$ calcd for $C_{19}H_{28}N_4O_3S_3$: 457.1396; found: 457.1389.

*4.1.1.3.3. 2-Oxo-2-((4-sulfamoylphenyl)amino)ethyl 4-(4-nitrophenyl)piperazine-1-carbodithioate (**3c**).* Yield: 82%, M.P. = 209–211 °C. ^{1}H NMR (300 MHz, DMSO-d_6): δ = 3.73 (4H, br.s., piperazine), 4.17 (4H, br.s., piperazine), 4.34 (2H, s, $-CH_2-$), 6.95 (2H, d, *J* =9.5 Hz, 1,4-Disubstitutedbenzene), 7.25 (2H, s, $-SO_2NH_2$), 7.75 (4H, d, *J* =2.3 Hz, 1,4-Disubstitutedbenzene), 8.10 (2H, d, *J* =9.4 Hz, 1,4-Disubstitutedbenzene), 10.63 (1H, br.s., –NH). ^{13}C NMR (75 MHz, DMSO-d_6): δ = 41.60, 45.17, 48.90, 50.59, 112.31, 119.08, 126.26, 127.21, 137.33, 138.92, 142.32, 154.16, 166.34, 195.12. HRMS (*m*/*z*): $[M+H]^+$ calcd for $C_{19}H_{21}N_5O_5S_3$: 496.0778; found: 496.0779.

*4.1.1.3.4. 2-Oxo-2-((4-sulfamoylphenyl)amino)ethyl 4-(4-fluorobenzyl)piperazine-1-carbodithioate (**3d**).* Yield: 86%, M.P. = 182–184 °C. ^{1}H NMR (300 MHz, DMSO-d_6): δ = 2.45–2.48 (4H, m, piperazine), 3.52 (2H, s, $-CH_2-$), 3.96 (2H, br.s., piperazine), 4.22 (2H, br.s., piperazine), 4.29 (2H, s, $-CH_2-$), 7.13–7.19 (2H, m, 1,4-Disubstitutedbenzene), 7.25 (2H, s, $-SO_2NH_2$), 7.36 (2H, dd, J_1 = 5.7 Hz, J_2 = 8.6 Hz, 1,4-Disubstitutedbenzene), 7.75 (4H, d, *J* = 2.6 Hz, 1,4-Disubstitutedbenzene), 10.62 (1H, br.s., –NH). ^{13}C NMR (75 MHz, DMSO-d_6): δ = 41.70, 50.27, 51.59, 52.28, 60.77, 115.45 (*J* = 21.0 Hz), 119.06, 127.19, 131.29 (*J* = 7.9 Hz), 134.18, 138.90, 142.34, 161.84 (*J* = 241.1 Hz), 166.41, 194.75. HRMS (*m*/*z*): $[M+H]^+$ calcd for $C_{20}H_{23}FN_4O_3S_3$: 483.0989; found: 483.0989.

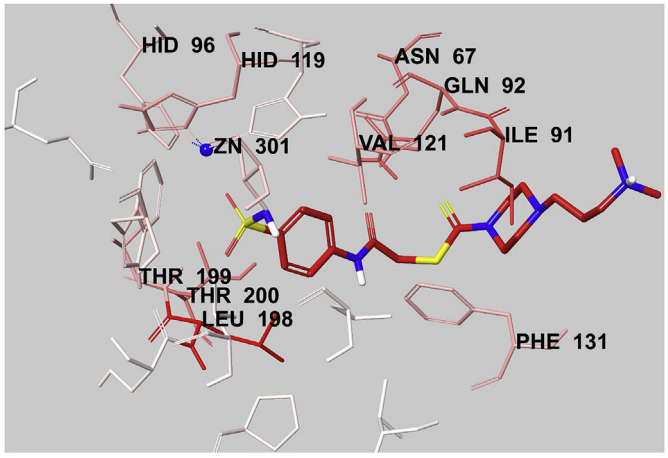

Fig. 11. The van der Waals interaction of compound **3h** with active region of *h*CA II. The active ligand has a lot of favorable van der Waals interactions (red and pink). (For interpretation of the references to color in this figure legend, the reader is referred to the Web version of this article.)

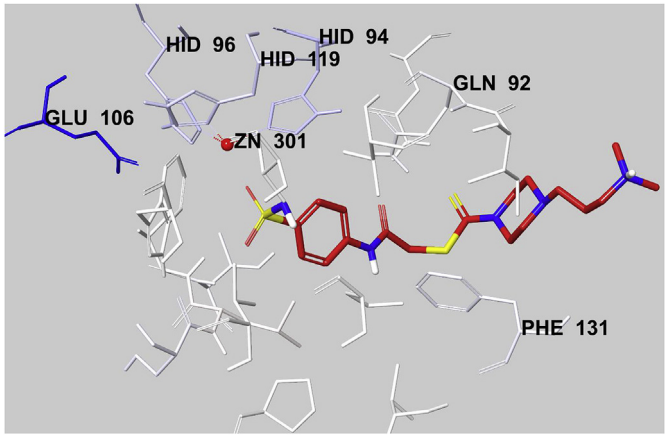

Fig. 12. The electrostatic interaction of compound **3h** with active region of *h*CA II. The residues are colored (blue and light blue) according to the distance from ligand by Per-Residue Interaction panel. (For interpretation of the references to color in this figure legend, the reader is referred to the Web version of this article.)

*4.1.1.3.5. 2-Oxo-2-((4-sulfamoylphenyl)amino)ethyl 4-(4-methylbenzyl)piperazine-1-carbodithioate (**3e**).* Yield: 81%, M.P. = 197–199 °C. ^{1}H NMR (300 MHz, DMSO-d_6): δ = 2.28 (3H, s, $-CH_3$), 2.46 (4H, br.s., piperazine), 3.49 (2H, s, $-CH_2$-), 3.95 (2H, br.s., piperazine), 4.21 (2H, br.s., piperazine), 4.29 (2H, s, $-CH_2$-), 7.14 (2H, d, J = 7.9 Hz), 7.20 (2H, d, J = 7.9 Hz), 7.26 (2H, s, $-SO_2NH_2$), 7.72–7.79 (4H, m, 1,4-Disubstitutedbenzene), 10.63 (1H, br.s., –NH). ^{13}C NMR (75 MHz, DMSO-d_6): δ = 21.19, 41.72, 50.29, 51.60, 52.31, 61.47, 119.07, 127.20, 129.29, 129.44, 134.77, 136.69, 138.90, 142.35, 166.42, 194.70. HRMS (*m*/*z*): $[M+H]^+$ calcd for $C_{21}H_{26}N_4O_3S_3$: 479.1240; found: 479.1233.

*4.1.1.3.6. 2-Oxo-2-((4-sulfamoylphenyl)amino)ethyl 4-(4-methoxybenzyl)piperazine-1-carbodithioate (**3f**).* Yield: 79%, M.P. = 205–207 °C. ^{1}H NMR (300 MHz, DMSO-d_6): δ = 2.43–2.46 (4H, br.s., piperazine), 3.46 (2H, s, –CH2-), 3.74 (3H, s, $-OCH_3$), 3.95 (2H, br.s., piperazine), 4.21 (2H, br.s., piperazine), 4.29 (2H, s, $-CH_2$-), 6.89 (2H, d, J = 8.6 Hz), 7.23 (2H, d, J = 8.7 Hz), 7.25 (2H, s, $-SO_2NH_2$), 7.75 (4H, d, J = 2.9 Hz, 1,4-Disubstitutedbenzene), 10.61 (1H, br.s., –NH). 13C NMR (75 MHz, DMSO-d_6): δ = 41.70, 50.35, 51.62, 52.26, 55.49, 61.15, 114.09, 119.07, 127.20, 129.73, 130.69, 138.90, 142.34, 158.89, 166.42, 194.66. HRMS (*m*/*z*): $[M+H]^+$ calcd for $C_{21}H_{26}N_4O_4S_3$: 495.1189; found: 495.1197.

*4.1.1.3.7. 2-Oxo-2-((4-sulfamoylphenyl)amino)ethyl-4-(2-(dimethylamino)ethyl)piperazine-1-carbodithioate (**3g**).* Yield: 75%, M.P. = 198–200 °C. ^{1}H NMR (300 MHz, DMSO-d_6): δ = 2.16 (6H, s, $-CH_3$), 2.39–2.41 (2H, m, $-CH_2$-), 2.43–2.45 (2H, m, $-CH_2$-), 2.51–2.53 (4H, br.s., piperazine), 3.94 (2H, br.s., piperazine), 4.19 (2H, br.s., piperazine), 4.29 (2H, s, $-CH_2$-), 7.25 (2H, s, $-SO_2NH_2$), 7.74 (4H, d, J = 2.3 Hz, 1,4-Disubstitutedbenzene), 10.62 (1H, br.s., –NH). ^{13}C NMR (75 MHz, DMSO-d_6): δ = 41.66, 45.85, 50.32, 51.62, 52.87, 55.33, 56.93, 119.06, 127.19, 138.90, 142.34, 166.42, 194.63. HRMS (*m*/*z*): $[M+H]^+$ calcd for $C_{17}H_{27}N_5O_3S_3$: 446.1349; found: 446.1329.

*4.1.1.3.8. 2-Oxo-2-((4-sulfamoylphenyl)amino)ethyl-4-(3-(dimethylamino)propyl)piperazine-1-carbodithioate (**3h**).* Yield: 84%, M.P. = 185–187 °C. ^{1}H NMR (300 MHz, DMSO-d_6): δ = 1.82–1.87 (2H, m, $-CH_2$-), 2.41 (2H, t, J = 6.7 Hz), 2.71 (6H, s, $-CH_3$), 3.01–3.06 (2H, m, $-CH_2$-), 3.35 (4H, br.s., piperazine), 3.97 (2H, br.s., piperazine), 4.21 (2H, br.s., piperazine), 4.31 (2H, s, $-CH_2$-), 7.26 (2H, s, $-SO_2NH_2$), 7.75 (4H, br.s., 1,4-Disubstitutedbenzene), 10.76 (1H, br.s., –NH). ^{13}C NMR (75 MHz, DMSO-d_6): δ = 21.37, 41.66, 42.52, 50.19, 51.47, 52.31, 54.26, 55.46, 119.04, 127.18, 138.87, 142.39, 166.43, 194.83. HRMS (*m*/*z*): $[M+H]^+$ calcd for $C_{18}H_{29}N_5O_3S_3$: 460.1505; found: 460.1492.

*4.1.1.3.9. 2-Oxo-2-((4-sulfamoylphenyl)amino)ethyl 4-(furan-2-carbonyl)piperazine-1-carbodithioate (**3i**).* Yield: 89%, M.P. = 221–223 °C. ^{1}H NMR (300 MHz, DMSO-d_6): δ = 3.87 (4H, br.s., piperazine), 4.11 (2H, br.s., piperazine), 4.26 (2H, br.s., piperazine), 4.33 (2H, s, $-CH_2$-), 6.60 (1H, dd, J_1 = 1.7 Hz, J_2 = 3.5 Hz, Furan), 7.08 (1H, dd, J_1 = 0.7 Hz, J_2 = 3.5 Hz, Furan), 7.25 (2H, s, $-SO_2NH_2$), 7.75 (4H, d, J = 2.4 Hz, 1,4-Disubstitutedbenzene), 7.87 (1H, dd, J_1 = 0.7 Hz, J_2 = 1.7 Hz, Furan), 10.63 (1H, br.s., –NH). ^{13}C NMR (75 MHz, DMSO-d_6): δ = 41.66, 43.95, 49.46, 50.92, 111.91, 116.62, 119.08, 127.21, 138.92, 142.33, 145.59, 147.10, 158.95, 166.35, 195.34. HRMS (*m*/*z*): $[M+H]^+$ calcd for $C_{18}H_{20}N_4O_5S_3$: 469.0669; found: 469.0659.

*4.1.1.3.10. 2-Oxo-2-((4-sulfamoylphenyl)amino)ethyl 4-(pyridin-2-yl)piperazine-1-carbodithioate (**3j**).* Yield: 77%, M.P. = 172–174 °C. ^{1}H NMR (300 MHz, DMSO-d_6): δ = 3.69 (4H, br.s., piperazine), 4.10 (2H, br.s., piperazine), 4.27 (2H, br.s., piperazine), 4.33 (2H, s, $-CH_2$-), 6.68 (1H, dd, J_1 = 5.0 Hz, J_2 = 6.7 Hz, Pyridine), 6.82 (1H, d, J = 8.6 Hz, Pyridine), 7.25 (2H, s, $-SO_2NH_2$), 7.57 (1H, td, J_1 = 1.9 Hz, J_2 = 7.1 Hz, Pyridine), 7.76 (4H, d, J = 1.9 Hz, 1,4-Disubstitutedbenzene), 8.13–8.15 (1H, m, Pyridine), 10.63 (1H, br.s., –NH). ^{13}C NMR (75 MHz, DMSO-d_6): δ = 41.65, 44.07, 49.73, 51.13, 107.44, 113.79, 119.09, 127.21, 138.17, 138.91, 142.34, 148.06, 158.61, 166.40, 194.99. HRMS (*m*/*z*): $[M+H]^+$ calcd for $C_{18}H_{21}N_5O_3S_3$: 452.0879; found: 452.0882.

*4.1.1.3.11. 2-Oxo-2-((4-sulfamoylphenyl)amino)ethyl 4-(pyrimidin-2-yl)piperazine-1-carbodithioate (**3k**).* Yield: 79%, M.P. = 187–189 °C. 1H NMR (300 MHz, DMSO-d_6): δ = 3.89 (4H, br.s., piperazine), 4.11 (2H, br.s., piperazine), 4.27 (2H, br.s., piperazine), 4.33 (2H, s, $-CH_2$-), 6.70 (1H, t, J = 4.7 Hz, Pyrimidine), 7.25 (2H, s, $-SO_2NH_2$), 7.76 (4H, d, J = 1.9 Hz, 1,4-Disubstitutedbenzene), 8.41 (2H, d, J = 4.7 Hz, Pyrimidine), 10.63 (1H, br.s., –NH). ^{13}C NMR (75 MHz, DMSO-d_6): δ = 41.68, 42.96, 49.80, 51.19, 111.12, 119.09, 127.21, 138.91, 142.33, 158.48, 161.29, 166.39, 195.12 HRMS (*m*/*z*): $[M+H]^+$ calcd for $C_{17}H_{20}N_6O_3S_3$: 453.0832; found: 453.0812.

4.2. Biological activity

4.2.1. Purification of CA isozymes from human erythrocytes by affinity chromatography

The erythrocytes were purified from fresh human blood obtained from the Blood Center of Ataturk University. The purification of the CA isozymes from the human erythrocytes by affinity

chromatography was performed as described in the previous study of the authors of the present study. All procedures were performed at 4 °C [13,36].

4.2.2. Measurement of CA activity

The hydratase activity assay was carried out according to the Wilbur-Anderson method [37].

The assay of the esterase activity of the human erythrocyte CA was carried out according to the method described by Verpoorte et al. [38]. Accordingly, by measuring the change in the absorbance of the 4-nitrophenyl acetate to the 4-nitrophenolate ion at 348 nm of over a period of 3 min at 25 °C using a spectrophotometer.

4.2.3. Inhibition assays

The inhibitory effects of the newly synthesized compounds on the CA enzyme activity were tested in triplicate for each concentration used. The compounds were tested at 10^{-3}-10^{-9} M concentrations. The IC_{50} values were calculated for the compounds at different concentrations by utilizing the graphs of activity %. The activities of the enzymes in the medium without inhibitors were used as 100% activity. The IC_{50} values were calculated from the plots of percentage enzyme activity versus the log of concentrations, and the regression analyses were computed in *GraphPad Prism Version 6*. The K_i values of the compounds were calculated by Lineweaver-Burk graphics [13].

4.2.4. Cytotoxicity test

The metabolic activity of viable cells was measured by MTT assay based on the reduction of 3-(4,5-dimethylthiazol-2-yl)-2,5-diphenyltetrazolium salt to formazan product, which can be quantified spectrophotometrically to determine the percentage of viable cells. The anticancer activity of the compounds (**3a-3k**) were screened according to the MTT assay using the NIH3T3 cell line. The MTT assay were performed as previously described [39–41].

4.3. Molecular docking

A docking study was performed to investigate the binding modes of compound **3h** to the *h*CA I and II enzyme active sites by using *in silico* procedure. The X-ray crystal structures of *h*CA I (PDB ID: 1AZM) [27] and *h*CA II (PDB ID: 3HS4) [28] were retrieved from the Protein Data Bank server (www.pdb.org). The docking procedure was applied as previously described by the research group of the present study [13].

Appendix A. Supplementary data

Supplementary data to this article can be found online at https://doi.org/10.1016/j.ejmech.2020.112392.

References

[1] D. Moi, A. Nocentini, A. Deplano, G. Balboni, C.T. Supuran, V. Onnis, Eur. J. Med. Chem. 182 (2019) 111638.
[2] A.S. El-Azab, A.A. Abdel-Aziz, S. Bua, A. Nocentini, M.M. Alanazi, N.A. AlSaif, I.A. Al-Suwaidan, M.M. Hefnawy, C.T. Supuran, Bioorg. Chem. 92 (2019) 103225.
[3] D. Tanini, L. Ricci, A. Capperucci, L. Di Cesare Mannelli, C. Ghelardini, T.S. Peat, F. Carta, A. Angeli, C.T. Supuran, Eur. J. Med. Chem. 181 (2019) 111586.
[4] M. Bozdag, M. Ferraroni, C. Ward, F. Carta, S. Bua, A. Angeli, S.P. Langdon, I.H. Kunkler, A.S. Al-Tamimi, C.T. Supuran, Eur. J. Med. Chem. 182 (2019) 111600.
[5] L. Vats, R. Kumar, S. Bua, A. Nocentini, P. Gratteri, C.T. Supuran, P.K. Sharma, Eur. J. Med. Chem. 183 (2019) 111698.
[6] B. Zengin Kurt, F. Sonmez, D. Ozturk, A. Akdemir, A. Angeli, C.T. Supuran, C.T., Eur. J. Med. Chem. 183 (2019) 111702.
[7] M.F. Abo-Ashour, W.M. Eldehna, A. Nocentini, A. Bonardi, S. Bua, H.S. Ibrahim, M.M. Elaasser, V. Krystof, R. Jorda, P. Gratteri, S.M. Abou-Seri, C.T. Supuran, Eur. J. Med. Chem. 184 (2019) 111768.
[8] B. Swain, C. Singh Digwal, A. Angeli, M. Alvala, P. Singh, C.T. Supuran, M. Arifuddin, Bioorg. Med. Chem. 27 (21) (2019) 115090.
[9] A. Aspatwar, N.K. Parvathaneni, H. Barker, E. Anduran, C.T. Supuran, L. Dubois, P. Lambin, S. Parkkila, J.Y. Winum, J. Enzym. Inhib. Med. Chem. 35 (1) (2020) 109–117.
[10] A.S. El-Azab, A.A. Abdel-Aziz, S. Bua, A. Nocentini, M.A. El-Gendy, M.A. Mohamed, T.Z. Shawer, N.A. AlSaif, C.T. Supuran, Bioorg. Chem. 87 (2019) 78–90.
[11] T. Akram, M.A. Abbasi, A. Mahmood, E. Barboza de Lima, F. Perveen, M. Ashraf, I. Ahmad, S. Goumri-Said, J. Mol. Struct. 1195 (2019) 119–130.
[12] V. Sharma, R. Kumar, S. Bua, C.T. Supuran, P.K. Sharma, P.K., Bioorg. Chem. 85 (2019) 198–208.
[13] B.N. Saglik, U. Acar Cevik, D. Osmaniye, S. Levent, B.K. Cavusoglu, B.K., Y. Demir, S. Ilgin, Y. Ozkay, A.S. Koparal, S. Beydemir, Z.A. Kaplancikli, Bioorg. Chem. 91 (2019) 103153.
[14] A.A. Abdel-Aziz, A.S. El-Azab, S. Bua, A. Nocentini, M.A. Abu El-Enin, M.M. Alanazi, N.A. AlSaif, M.M. Hefnawy, C.T. Supuran, Bioorg. Chem. 87 (2019) 425–431.
[15] D. Tanini, A. Capperucci, M. Scopelliti, A. Milaneschi, A. Angeli, C.T. Supuran, Bioorg. Chem. 89 (2019) 102984.
[16] C. Yamali, H.I. Gul, A. Ece, S. Bua, A. Angeli, H. Sakagami, E. Sahin, C.T. Supuran, Bioorg. Chem. 92 (2019) 103222.
[17] W.M. Eldehna, M.A. Abdelrahman, A. Nocentini, S. Bua, S.T. Al-Rashood, G.S. Hassan, A. Bonardi, A.A. Almehizia, H.M. Alkahtani, A. Alharbi, P. Gratteri, C.T. Supuran, Bioorg. Chem. 90 (2019) 103102.
[18] N. Chiaramonte, S. Bua, A. Angeli, M. Ferraroni, L. Picchioni, G. Bartolucci, L. Braconi, S. Dei, E. Teodori, C.T. Supuran, M.N. Romanelli, Bioorg. Chem. 91 (2019) 103130.
[19] A. Angeli, L. Di Cesare Mannelli, C. Ghelardini, T.S. Peat, G. Bartolucci, M. Menicatti, F. Carta, C.T. Supuran, Eur. J. Med. Chem. 177 (2019) 188–197.
[20] N. Lolak, S. Akocak, S. Bua, R.K.K. Sanku, C.T. Supuran, C.T., Bioorg. Med. Chem. 27 (8) (2019) 1588–1594.
[21] M. Bozdag, F. Carta, D. Vullo, A. Akdemir, S. Isik, C. Lanzi, A. Scozzafava, E. Masini, C.T. Supuran, Bioorg. Med. Chem. 23 (10) (2015) 2368–2376.
[22] F. Carta, M. Aggarwal, A. Maresca, A. Scozzafava, R. McKenna, C.T. Supuran, Chem. Commun. 48 (13) (2012) 1868–1870.
[23] M. Bozdag, F. Carta, D. Vullo, S. Isik, Z. AlOthman, S.M. Osman, A. Scozzafava, C.T. Supuran, J. Enzym. Inhib. Med. Chem. 31 (1) (2016) 132–136.
[24] S. Avram, A.L. Milac, F. Carta, C.T. Supuran, J. Enzym. Inhib. Med. Chem. 28 (2) (2013) 350–359.
[25] N.V. Bhagavan, first ed., Elsevier, Burlington, MA, USA, 2011, pp. 47–58.
[26] International Organization for Standardization, Biological Evaluation of Medical Devices-Part 5: Tests for in Vitro Cytotoxicity, third ed., 2009. ISO-10993-5.
[27] S. Chakravarty, K.K. Kannan, J. Mol. Biol. 243 (1994) 298–309.
[28] K.H. Sippel, A.H. Robbins, J. Domsic, C. Genis, M. Agbandje-McKenna, R. McKenna, Acta Crystallogr. Sect. F. Struct. Biol. Cryst. Commun. 65 (2009) 992–995.
[29] R.W. King, A.S. Burgen, Biochim. Biophys. Acta 207 (1970) 278–285.
[30] F. Abbate, C.T. Supuran, A. Scozzafava, P. Orioli, M.T. Stubbs, G. Klebe, J. Med. Chem. 45 (2002) 3583–3587.
[31] F. Pacchiano, F. Carta, P.C. McDonald, Y. Lou, D. Vullo, A. Scozzafava, S. Dedhar, V.T. Supuran, J. Med. Chem. 54 (2011) 1896–1902.
[32] J. Ivanova, A. Balode, R. Žalubovskis, J. Leitans, A. Kazaks, D. Vullo, K. Tars, C.T. Supuran, Bioorg. Med. Chem. 25 (2017) 857–863.
[33] J. Leitans, A. Sprudza, M. Tanc, I. Vozny, R. Zalubovskis, K. Tars, C.T. Supuran, Bioorg. Med. Chem. 21 (2013) 5130–5138.
[34] B.S. Avvaru, J.M. Wagner, A. Maresca, A. Scozzafava, A.H. Robbins, C.T. Supuran, R. McKenna, Bioorg. Med. Chem. Lett 20 (2010) 4376–4381.
[35] Glide, Schrödinger, LLC, New York, NY, 2016 version 7.1.
[36] S. Mert, Z. Alım, M.M. İşgör, B. Anıl, R. Kasımoğulları, Ş. Beydemir, Arab. J. Chem. 12 (8) (2019) 2740–2748.
[37] K.M. Wilbur, N.G. Anderson, J. Biol. Chem. 176 (1) (1948) 147–154.
[38] J.A. Verpoorte, S. Mehta, J.T. Edsall, J. Biol. Chem. 42 (1967) 4221–4229.
[39] M.V. Berridge, P.M. Herst, A.S. Tan, Biotechnol. Annu. Rev. 11 (2005) 127–152.
[40] Ü. Demir Özkay, Ö.D. Can, B.N. Sağlık, U.A. Çevik, S. Levent, Y. Özkay, S. Ilgın, Ö. Atlı, Bioorg. Med. Chem. Lett 26 (22) (2016) 5387–5394.
[41] D. Osmaniye, S. Levent, C.M. Ardıç, Ö. Atlı, Y. Özkay, Z.A. Kaplancıklı, Phosphorus, Sulfur Silicon Relat. Elem. 193 (4) (2018) 249–256.